Multiple Structure-Reactivity Correlations in the Hydrolysis of Epimeric 2-(Aryloxy)-2-oxydioxaphosphorinanes. Stereoelectronic Effects

Robert Rowell and David G. Gorenstein*[1]

Contribution from the Department of Chemistry, University of Illinois Chicago Circle, Chicago, Illinois 60680. *Received February 25, 1981*

Abstract: The epimeric 2-(aryloxy)-2-oxo-*trans*-5,6-tetramethylene-1,3,2-dioxaphosphorinanes **1**–**4** (ArO = *p*-methoxyphenoxy, *p*-nitrophenoxy, phenoxy, and 2,4-dinitrophenoxy) and isomeric 2-(*p*-nitrophenoxy)-2-oxo-*trans*-5,6-tetramethylene-1,3,2-oxazaphosphorinane (**5**) were hydrolyzed in 30% dioxane/water at 70 °C with a variety of nucleophiles. The reactivities were sensitive to changes in both the nucleophile and leaving group. The Brønsted β_{nuc}'s for the equatorial leaving groups 2,4-DNP, PNP, and Ph are 0.48, 0.64, and 0.75, respectively. The Brønsted β_{lg}'s are −0.96, −1.04, −0.85, −0.66, −0.64, −0.57, −0.46, and −0.35 for nucleophiles water, methoxyacetate, acetate, phosphate, hexafluoroisopropoxide, carbonate, trifluoroethoxide, and hydroxide, respectively, for the equatorial triesters. These results are best interpreted in terms of a change in mechanism from a concerted $S_N2(P)$ process to a stepwise one. The stepwise mechanism via a pentacovalent intermediate is supported by the stereochemistry of reaction and epimeric rate ratios. Thus, some retention of configuration at phosphorus was observed in the methanolysis of all triesters except **4b** and **5b**. Also the hydroxide-catalyzed hydrolysis of **4a** and **1b** yielded some retention at phosphorus, and, therefore, a pentacovalent intermediate is required for attack by very basic nucleophiles. This agrees with the kinetic results if one considers the fact that β_{lg} for hydroxide is only 0.35. Solvent deuterium isotope effects, k_{H_2O}/k_{D_2O}, for acetate-catalyzed hydrolysis of the dinitrophenyl triesters were determined to be 1.08. Thus, these triesters hydrolyze mostly via nucleophilic catalysis. The isotope effects for phosphate-catalyzed hydrolysis of the equatorial *p*-nitrophenyl and phenyl triesters are 1.19 and 1.8, respectively. This indicates an increasing amount of hydrolysis via general-base catalysis toward the poorer leaving groups.

The role of the pentacovalent phosphorus intermediate in the reactions of phosphate triesters has continued to be a subject of controversy. The question whether the hydrolysis of triesters proceeds via a true metastable intermediate in a two-step, addition–elimination mechanism or through a concerted $S_N2(P)$ mechanism without formation of a pentacovalent intermediate still remains unravelled.[2-10] The studies on reactions of cyclic five-membered ring phosphate esters have been very productive and have yielded powerful evidence for reaction via a trigonal-bipyramidal intermediate which may further pseudorotate.[2] The five-membered ring imparts certain constraints to the reaction pathway which may or may not permit extrapolation of this pathway to that of six-membered rings or acyclic esters.

In addition, the hydrolysis of trisubstituted phosphoric acid esters may be subject to general-base catalysis as well as nucleophilic catalysis, depending on the nature of the substituents, the nucleophiles, and the leaving groups. A change in hydrolysis mechanism from nucleophilic to general-base catalysis as the nucleophile becomes markedly less basic than the leaving group has been demonstrated in a number of cyclic triesters.[4]

In the present study we examine the reaction mechanism of a series of epimeric substituted aryl triesters. This is the first kinetic investigation of epimeric isomers and differences in reactivity as well as reaction stereochemical information have provided the first set of data consistent with a change in mechanism from a concerted process to a stepwise one. Finally, this study further extends Lehn and Wipff's[11] and Gorenstein et al.'s[12-17] work on the nature of stereoelectronic effects in the reactions of phosphate esters.

Experimental Section

^1H and ^{31}P NMR spectra were recorded on a Bruker WP-80 spectrometer at 80 and 32.4 MHz, respectively, or ^1H NMR on a 60-MHz Varian T-60 spectrometer. High-field ^{31}P NMR spectra were recorded on Nicolet NTC-200 or NTC-360 spectrometer. Chemical shifts in parts per million (ppm) for ^1H NMR spectra are referenced to internal Me_4Si and for ^{31}P NMR spectra are referenced to external 85% H_3PO_4. Mass spectra were obtained on an AEI/MS 30 spectrometer. Melting points were obtained on a Thomas Hoover apparatus and are uncorrected. Repetitive scan spectra were taken on a Cary 210 spectrometer.

Materials. Doubly distilled water was used in all buffer solutions. *p*-Dioxane was purified by the procedure of Riddick and Bunger[18] and stored frozen under argon prior to use. No peroxides were detected by KI/starch paper from any dioxane stored in this way. All chemicals and solvents were commercially available reagent grade materials. Inorganic salts were used without purification. Most buffer acids were used newly purchased or purified. D_2O was obtained from Stohler Isotopes Co. (99.8% D).

2-(Aryloxy)-2-oxo-*trans*-5,6-tetramethylene-1,3,2-dioxaphosphorinane (2-(Aryloxy)-1,3-dioxa-2-phospha-*trans*-decalin-2-one) (1a,b–4a,b). These compounds were prepared as described in ref 17a,b. Compounds labeled **a** are axial and those labeled **b** are "equatorial", assuming a chair conformation. Aryloxy substituents are *p*-methoxyphenoxy (PMP),

(1) Alfred P. Sloan Fellow.
(2) Westheimer, F. H. *Acc. Chem. Res.* **1968**, *1*, 70.
(3) Mislow, K. *Acc. Chem. Res.* **1970**, *3*, 321.
(4) Kahn, S. A.; Kirby, A. J. *J. Chem. Soc. B* **1970**, 1172.
(5) Lazarus, R. A.; Benkovic, S. J. *J. Am. Chem. Soc.* **1979**, *101*, 4300.
(6) Boudreau, J. A.; Brown, C.; Hudson, R. F. *J. Chem. Soc., Chem. Commun.* **1975**, 679.
(7) Bauman, M.; Wadsworth, W. S., Jr. *J. Am. Chem. Soc.* **1978**, *100*, 6388.
(8) (a) Inch, T. D.; Lewis, G. J.; Wilkinson, R. G.; Watts, P. *J. Chem. Soc., Chem. Commun.* **1975**, *13*, 500. (b) Harrison, J. M.; Inch, T. D.; Lewis, G. J. *J. Chem. Soc. B* **1974**, 1053.
(9) (a) Bunton, C. A. *Acc. Chem. Res.* **1970**, *3*, 257. (b) Gillespie, P.; Ramirez, F.; Ugi, I.; Marquarding, D. *Angew. Chem., Int. Ed. Eng.* **1973**, *12*, 91. (c) McEwen, W. E.; Berlin, K. D., Eds. "Organophosphorus Stereochemistry, Parts I and II"; Dowden, Hutchinson and Ross: Stroudsburg, Pennsylvania, 1975. (d) Hudson, R. F.; Brown, C. *Acc. Chem. Res.* **1972**, *5*, 204.
(10) Gorenstein, D. G.; Lee, Y. G. *J. Am. Chem. Soc.* **1978**, *99*, 2258.
(11) Lehn, J. M.; Wipff, G. *J. Chem. Soc., Chem. Commun.* **1975**, 800.
(12) Gorenstein, D. G.; Findlay, J. B.; Luxon, B. A.; Kar, D. *J. Am. Chem. Soc.* **1977**, *99*, 3473.
(13) Gorenstein, D. G.; Luxon, B.; Findlay, J. B.; Momii, R. *J. Am. Chem. Soc.* **1977**, *99*, 4170.
(14) Gorenstein, D. G.; Luxon, B. A.; Findlay, J. B. *J. Am. Chem. Soc.* **1977**, *99*, 8048.
(15) Gorenstein, D. G.; Luxon, B. A.; Findlay, J. B. *J. Am. Chem. Soc.* **1979**, *101*, 5869.
(16) Gorenstein, D. G.; Luxon, B. A.; Goldfield, E. *J. Am. Chem. Soc.* **1980**, *102*, 1757.
(17) (a) Gorenstein, D. G.; Rowell, R.; Findlay, J. *J. Am. Chem. Soc.* **1980**, *102*, 5077. (b) Gorenstein, D. G.; Rowell, R. *J. Am. Chem. Soc.* **1979**, *101*, 4925.
(18) Riddick, J. A.; Bunger, W. B. "Techniques of Chemistry", Vol. II, "Organic Solvents", 1970, Wiley: New York, pp 706–710.

0002-7863/81/1503-5894$01.25/0

phenoxy (P), *p*-nitrophenoxy (PNP), and 2,4-dinitrophenoxy (2,4-DNP) for compounds labeled **1** through 4, respectively.

2-(*p*-Nitrophenoxy)-2-oxo-*trans*-5,6-tetramethylene-1,3,2-oxazaphosphorinane (2-*p*-Nitrophenoxy-1,3-oxaza-2-phospha-*trans*-decalin-2-one) (5a,b). These were prepared as in ref 17.

Dissociation Constants and pH Measurements. pK_a determinations were made from several buffer acid–base ratios or triplicate measurements at one ratio at 70 °C, 30% dioxane/water (v/v), buffer concentration of 0.1 M, and ionic strength of 1.0 M maintained with KCl. Measurements were made on a Radiometer PHM26 with a type G222C or G222B semimicroelectrode and type 4112 KCl electrode. Measurements in 30% dioxane/D_2O were calculated from the equation pK = pH (meter reading) + 0.29.[19] The dissociation constant of water in 30% dioxane/water was obtained by extrapolation of the data in ref 20 to both 30% dioxane and 70 °C. The K_w is therefore approximately 1.6×10^{-14}. The pH meter was calibrated against standard buffers and readings are otherwise uncorrected. The pHs of stock solutions and pHs of cells after reaction were checked at room temperature. pH drift was generally less than ±0.03 pH unit. pHs of serially diluted buffers over an eightfold dilution ranged up to 0.1 pH unit.

Kinetics. Kinetic measurements were carried out on a Cary 16 UV–visible spectrophotometer equipped with an automatic sample changer and thermostated cuvette holder. Time vs. absorbance data was fed directly to a PDP 11/03 computer. The pseudo-first-order rate constants were determined by an iterative, nonlinear least-squares computer program.[10] Occasionally the computer-generated rate constant was checked against the slope of a ln $(A_\infty - A_t)$ vs. time plot. Most reactions were followed for at least 3 half-lives. With this data the computer program would iteratively fit the rate constant, initial absorbance, and final absorbance. The calculated and observed A_∞ generally agreed to within ±1%. Duplicate runs agreed within ±3%. Very slow reactions were followed by the method of initial rates. Here duplicate runs generally agreed to within ±10%.

Reactions were followed by measuring the rate of appearance of the particular phenoxide or phenol at a suitable wavelength. Compounds **1–5** all had significant differences in absorption curves between product phenol, and starting triester. In several cases confirmatory runs were carried out by following the disappearance of the triester. All reactions gave good first-order kinetics with the exception of **4a** with trifluoroethoxide which was biphasic. At a free-base buffer concentration of 0.01 M, pH 11.9, 24% of the reaction went by a second route. The rate constant of the initial fast reaction is attack at phosphorus. The second slower reaction has the same rate constant as the hydrolysis of (1,1,1-trifluoroethoxy)-2,4-dinitrobenzene in the same buffer. Thus, initially the trifluoroethoxide attacks both phosphorus and the aromatic carbon. The reaction of **2b** with hydronium ion gave an initial lag period and then proceeded with first-order kinetics. The lag period was probably due to oxidation of phenol by dissolved oxygen, and degassing the solution did shorten the lag period. Unless otherwise specified, kinetic runs were carried out at 70.7 °C in 30% dioxane/water (v/v) and ionic strength of 1.0 M maintained with KCl.

Second-order buffer-catalyzed rate constants were obtained as the slope from plots of k_{obsd} vs. free-base concentration. From 4 to 6 serially diluted buffer solutions were used at each pH. Catalysis by fluoride was determined by using tris buffer as was the acetate-catalyzed hydrolysis of the *p*-nitrophenyl esters. The buffer-catalyzed reaction was much faster than the tris reaction. The plots were linear with the exception of reactions where the acid component of the buffer was greater than 0.2 M. However, as dilutions were made and the concentration of the acid component became less than 0.2 M, the plots were linear and slopes were taken in this region. The acid component of the buffer acts in addition to dioxane to lower the rate. Repetitive scans were made on all isomers (except **1a** and **2a** in acid) hydrolyzed in acid and base. Sharp isosbestic points were obtained for all reactions (except **2b** in acid discussed earlier).

Product Analysis. Product analysis was made by ^{31}P NMR. The various isomers were not hydrolyzed exactly under kinetic conditions due to their limited solubility. Hydrolyses were generally done in 75% dioxane/water (v/v) with an ionic strength of 0.1 M. The isomer was typically dissolved in 300 μL of dioxane, and 100 μL of buffer was added such that the final concentrations were 0.05 and 0.1 M, respectively. Anions employed were hydroxide, trifluoroethoxide, acetate, and chloroacetate for triester **4a**. Acid hydrolyses were done on **4a**, **4b**, **3b**, **2a**, and **2b**. Fluoride was reacted with both **4a** and **4b**. In addition 4 and **4b** were reacted with acetate in methanol.

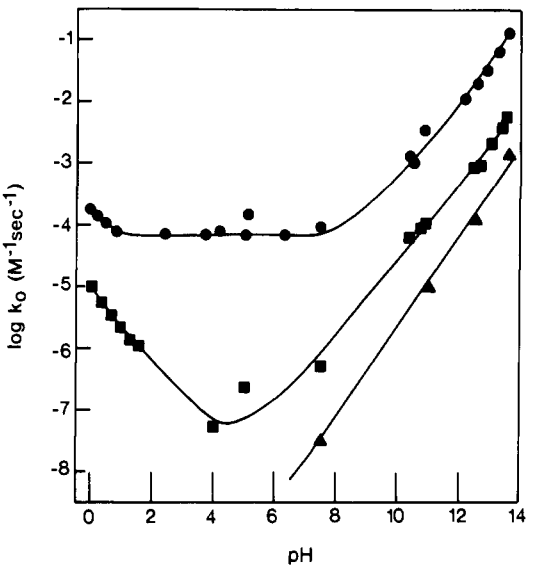

Figure 1. pH–rate profiles for **4a**, ●, **3a**, ■, and **2a**, ▲, at 70 °C, ionic strength 1.0 M (KCl), and 30% dioxane/water.

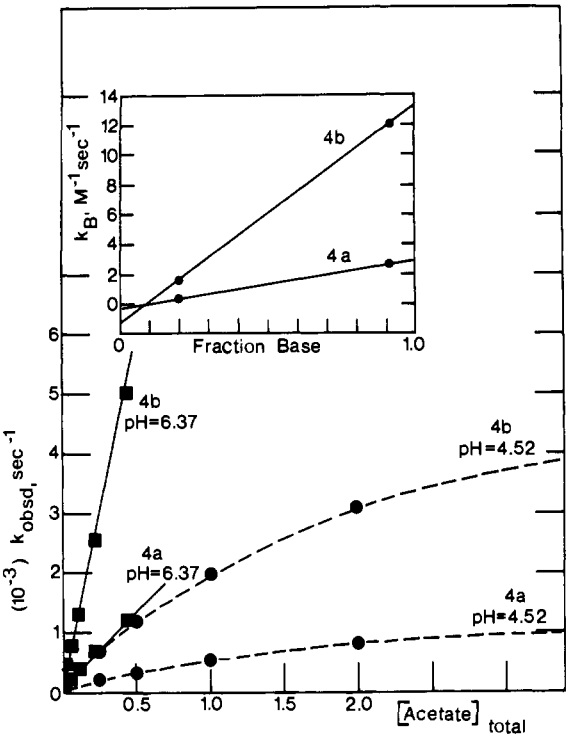

Figure 3. Dependence of the observed pseudo-first-order rate constants for the hydrolysis of **4a** annd **4b** on the concentration of acetic acid buffers.

P–O/C–O Cleavage. Reactions run with $H_3{}^{18}O^+$ were performed on **4a**, **4b**, and **2b**. Reactions with $^{18}OH^-$ were done on **4a**, **4b**, and **1b**. P–O vs. C–O cleavage was determined by comparing the ratio of $^{18}O/^{16}O$ in the product via ^{31}P NMR peak integration, by using the ^{18}O isotope shift on the ^{31}P chemical shift.[22-25] Additionally in the case of **4a**, unreacted starting material and product 2,4-dinitrophenol were analyzed by mass spectroscopy where the *m/e* ratios 314/312, 186/184, and 156/154 were used for ^{18}O-enrichment determination.

Results and Discussion

Lyate Species Catalysis. The dependence on pH of the first-order rate constants for hydrolysis in the absence of general acids

(19) Fife, T. H.; Bruice, T. C. *J. Phys. Chem.* **1961**, *65*, 1079.
(20) Harned, H. S.; Fallon, L. D. *J. Am. Chem. Soc.* **1939**, *61*, 2374.
(21) (a) Archie, W. G., Jr.; Westheimer, F. H. *Ibid.* **1973**, *95*, 5955. (b) Ramirez, F.; Nowakowski, M.; Maracek, J. *Ibid.* **1974**, *96*, 7269. (c) Skowronska, A.; Pakulski, M.; Michalski, J. *Ibid.* **1979**, *101*, 7412.
(22) Cohn, M.; Hu, A. *Proc. Natl. Acad. Sci. U.S.A.* **1978**, *75*, 200.
(23) Lowe, G.; Sproat, B. S. *J. Chem. Soc., Chem. Commun.* **1978**, 565.
(24) Lutz, O.; Nolle, A.; Staschewski, D. *Z. Naturforsch., A* **1978**, *33A*, 380.
(25) Gorenstein, D. G.; Rowell, R. *J. Am. Chem. Soc.* **1980**, *102*, 6165.

Table I. Enthalpies and Entropies of Activation

	bases							
	hydroxide		formate		hydroxide		hydroxide	
	4a[a]	4b[a]	4a[a]	4b[a]	2a[a]	2b[a]	5a[a]	5b[a]
$\Delta H^{\ddagger}$	12.9	10.0	17.3	14.8	15.6	13.5	11.9	10.9
$\Delta S^{\ddagger}$	−19.6	−23.1	−18.6	−24.5	−22.3	−25.5	−24.9	−25.0

[a] Isomers.

or bases (k_0) is shown in Figures 1 and 2 (see supplementary material) for the axial triesters **2a–4a** and equatorial triesters

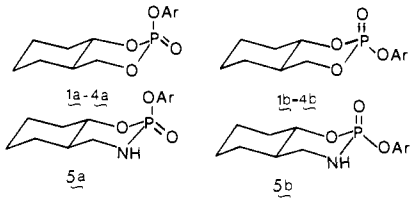

2b–4b, respectively. The results are consistent with the rate equations eq 1 and 2. Values of k_0 were obtained from the

$$k_0 = k_{H^+}[H^+] + k_{OH^-}[OH^-] + k_{H_2O}[H_2O] \quad (1)$$

$$k_{obsd} = k_0 + k_B[B] \quad (2)$$

intercepts of plots of k_{obsd} against total buffer concentration (Figure 3) or against free-base concentration (Figure 4; supplementary material). The pH–rate profile shows that the reaction is catalyzed by both hydronium and hydroxide ions. The more reactive isomers **4a** and **4b** (2,4-dinitrophenyl) show a significant water rate, but as the leaving group becomes poorer, the water rate becomes less important and the hydroxide- and hydronium-catalyzed reactions account for the entire reaction.[4] Compounds **4a** and **4b** both hydrolyze independent of pH between pH 2 and 7 with k_{H_2O} (38.8 M) = 6.6×10^{-5}. This same rate for water attack for both epimers (k_b/k_a = 1) may be contrasted with the hydroxide rate ratio, k_b/k_a, of 9.1 and the hydronium ion ratio of 5.1. Compounds **3a** and **3b** (*p*-nitrophenyl) show a similar effect in that the rate ratio k_b/k_a is 8.5 and 8.7 for k_{H^+} and K_{OH^-}, respectively, but only 3.7 for k_{H_2O}. The hydroxide ratio for **2b**/**2a** (phenyl) is 5.5 and for **1b**/**1a** (methoxyphenyl) is 5.4. For **5b**/**5a** the ratio is 3.0 for hydroxide and 6.1 for acid hydrolysis which involves P–N cleavage. The hydroxide ratios were determined at 70 °C and would be larger if done at lower temperatures. Thus k_b/k_a for **4** increases from 9.1 at 70 to 37.5 at 0 °C. Table I contains $\Delta H^{\ddagger}$ and $\Delta S^{\ddagger}$ for several reactions. In each case it is noted that the entropy of activation for the equatorial reaction is higher than that of the axial and that the $\Delta H^{\ddagger}$ is higher for the axial epimer.

Salt and Solvent Effects. Specific-salt effects were checked by substituting sodium nitrate for potassium chloride in the acetate-catalyzed reaction (10:1 buffer ratio, pH 5.22 for $NaNO_3$). The point for 1 M sodium acetate was slightly low for the KCl line and slightly high for the $NaNO_3$ line. The slopes differed in that the rate constant for the KCl salt solution was 12% faster for the axial **4a** and 22% faster for the equatorial **4b**. Thus specific-salt effects are minimal for this reaction. (In contrast to the results of Gorenstein and Lee.[10])

In changing solvent from 100% H_2O to 30% dioxane/water the rate of hydrolysis in general decreased (Table II), indicating inhibition by the organic component. It is interesting to note the relative change of the rates between the two isomers. Isomer **4a** hydrolyzed 3.4 times faster in going from 0.05 to 0.1 M ionic strength, but **4b** hydrolyzes 14 times faster. Thus, k_b/k_a for this ionic strength change increases from 4.6 to 19.2. Therefore, isomer **4b** is significantly more destabilized by this change in ionic strength.

Solvent deuterium isotope effects were studied in several of the reactions (Table III). The results for the acetate-catalyzed hydrolysis shows k_{H_2O}/k_{D_2O} of 1.07 and 1.08 for **4a** and **4b**, respectively. The isotope effect for phosphate-catalyzed hydrolysis of **3b** is 1.19 ± 0.1. The deuterium isotope effect for the much

Table II. Solvent and Ionic Strength Effects in the Hydrolysis of 4a and 4b in 0.01 M NaOH at 22 °C

	ionic strengths			
isomer	0.01	0.05[c]	0.10[c]	1.0[c]
	rate of hydrolysis			
4a[a]	5.87×10^{-4}	4.46×10^{-4}	1.53×10^{-3}	1.08×10^{-3}
4b[a]	1.62×10^{-3}	2.05×10^{-3}	2.93×10^{-2}	3.20×10^{-2}
4a[b]	1.40×10^{-3}		1.67×10^{-3}	1.30×10^{-3}
4b[b]	2.80×10^{-2}		2.73×10^{-2}	2.96×10^{-2}
	pH			
	7.74[a]	7.82[a]	11.95[a]	11.93[a]
	11.83[b]		11.95[b]	11.97[b]

[a] 30% dioxane/H_2O. [b] 100% H_2O. [c] KCl added to obtain ionic strength.

Table III. Conditions and Rate Constants for Hydrolysis in 30% Dioxane/D_2O, 70 °C, and μ = 1.0 KCl

nucleophile	isomer	condns	rate const	k_{H_2O}/k_{D_2O}
acetate	4a	0.05–0.4 M acetate, pD 6.74–6.77	2.81×10^{-4}	1.07
acetate	4b	0.05–0.4 M acetate, pD 6.74–6.77	1.20×10^{-2}	1.08
phosphate	2b	0.037–0.15 M HPO_4^{2-}, pD 7.90–8.34	2.18×10^{-6}	1.8
phosphate	3b	0.037–0.3 M HPO_4^{2-}, pD 7.90–8.34	1.91×10^{-4}	1.19
water	4a	1.0 M KCl, pD 8.1–5.2	4.34×10^{-5}	1.5
water	4b	1.0 M KCl, pD 8.1–5.2	4.37×10^{-5}	1.5

less reactive phenyl isomer **2b** is 1.8 ± 0.3. An isotope effect of 2.0 is generally believed to represent complete general-base catalysis in this type of system.[4] Thus the 2,4-dinitrophenyl esters hydrolyze exclusively via nucleophilic catalysis in an acetate buffer. When isomer **4a** was hydrolyzed in 0.1 M trifluoroethoxide (base/acid = 1/4) in 25% water/dioxane, no intermediate buildup of the trifluoroethoxy triester was observed. If the reaction was a nucleophilic displacement of 2,4-dinitrophenoxide, then a buildup of the trifluoroethoxy triester should have been observed. The pK_a of trifluoroethanol is 12.2, and the trifluoroethoxy triester should hydrolyze even slower than the phenoxy triester. Thus trifluoroethoxide may act as a general-base catalyst. The *p*-nitrophenyl ester hydrolyses via mostly nucleophilic catalysis and the phenyl ester mostly via general-base catalysis in phosphate buffers. This is consistent with the general trend in hydrolyses that as the pK of the nucleophile becomes much less than that of the leaving group, general-base catalysis becomes the preferred pathway. Thus also the spontaneous water reaction occurs with a deuterium isotope effect of 1.5 and is predominantly general-base catalysis for the 2,4-dinitrophenyl esters.

Products. The cyclic phosphate diester at −3.25 ppm was the only product observed via ^{31}P NMR in the hydrolysis of isomer **4a** by anions, hydroxide, trifluoroethoxide, acetate, and chloroacetate. Acid hydrolyses of isomers **4a**, **4b**, and **3b** also yielded only the protonated cyclic diester at −5.90 ppm. Base hydrolysis of **2a** yielded only the cyclic diester anion at −2.73 ppm at 70 °C. However, acid hydrolysis of **2a** yielded 73% cyclic diester at −5.87 ppm, 17% acyclic diester still esterified at the primary carbon oxygen at −6.29 ppm, and 10% still esterified to the secondary carbon oxygen at −7.16 ppm. Assignments were made by ob-

Table IV. Rate Constants for the Reactions of Epimer 2a

nucleophile	pK_a	concn range, M	pH	k_B	k_{hyd}
phosphate	6.73	0.037–0.3	7.56	4.83×10^{-7}	7.05×10^{-9}
HF isopropoxide	9.42	0.05–0.2	10.74	4.40×10^{-5}	8.76×10^{-6}
TF ethoxide	12.22	0.012–0.4	12.54	3.43×10^{-3}	1.21×10^{-4}
hydroxide	15.4	0.1–1.0		1.36×10^{-2}	

taining proton-coupled ^{31}P NMR spectra where the primary carbons' two protons split phosphorus into a triplet and the secondary's proton split phosphorus into a doublet of 6.3 Hz. The cyclic diester showed basically a doublet of triplets with the large coupling of 25.4 Hz. Isomer **2b** yielded 52% cyclic diester at −5.95 ppm, 14% diester esterified to the primary carbon oxygen at −6.34 ppm, and 35% diester still esterified to the secondary carbon oxygen at −7.19 ppm.

Isomer **2b** was also hydrolyzed in acid containing ^{18}O water. All three product peaks showed the same ^{18}O enrichment as in the solvent via ^{31}P NMR peak integration. Thus even ring opening involved P–O cleavage. Unreacted **2b** showed no detectable incorporation of ^{18}O (via ^{31}P NMR) after 40% reaction, so no evidence for an intermediate was obtained.

Other reactions in ^{18}O-enriched water such as hydroxide with **4a**, **4b**, and **1b** and acid with **4a** and **4b** showed the same $^{18}O/^{16}O$ ratio in the product diester as in the solution so that only P–O cleavage is involved. Unreacted **4a** and 2,4-dinitrophenol were analyzed by mass spectroscopy, and no evidence for ^{18}O incorporation was found since the M + 2/M peak ratio was the same as for the unenriched compounds. It is important to note that only one O-18 atom is incorporated into the diester product. This result rules out the possibility that the base-catalyzed reaction proceeds via a hexacovalent species as recently demonstrated for some displacement reactions of pentacovalent phosphoranes.[21] Thus if the phosphoryl oxygen and the two added solvent oxygens in a hexacovalent intermediate can permutationally exchange, then a fraction of the diester product should have two oxygen 18-atoms.

Fluoride reacted with **4b** to yield the axial fluorophosphate at −15.79 ppm and J_{P-F} of 1001 Hz. Fluoride reacted with **4a** to yield the equatorial fluorophosphate at −15.19 ppm and J_{P-F} of 983 Hz. Later spectra of the **4a** reaction showed formation of some axial fluorophosphate, but this was due to equilibration. Thus fluoride displaces 2,4-dinitrophenoxide with 100% inversion of configuration.

Acetate-catalyzed methanolysis was also carried out on **4a** and **4b**. Isomer **4a** yielded 27% equatorial methyl ester at −4.68 ppm and 73% of the cyclic diester at −2.44 ppm whereas **4b** yielded initially 22% of the axial methyl ester at −5.46 ppm and 78% cyclic diester at −2.59 ppm. Acetate acting as a nucleophilic catalyst would form the mixed anhydride which could be attacked either at carbon (as is known to occur for diesters[26a] and triesters[26b] to form the cyclic diester or at phosphorus to form the methyl triester. With the assumption that dinitrophenoxide is still displaced via inversion[17] and since the methyl triester is the single inversion product, it would be necessary to say that methanol displaced acetate with retention. Since acetate has a pK_a close to dinitrophenoxide, this would be unlikely. The 22–27% methyl triester could alternatively be formed from direct attack of methanol on the triester. Finally it is also possible that in methanol acetate could act as a general-base catalyst to form the inversion product. However, recent experiments (P. Abuaf, Z. Panosyan, D. Gorenstein, unpublished data) with ^{18}O-labeled acetate confirm that an oxygen from acetate is transferred to the diester product in unenriched water.

Buffer Catalysis. The second-order rate constants for base-catalyzed hydrolysis were obtained from the slopes of plots of k_{obsd} against the concentration of free base concentration of the buffer and are in Tables IV–VIII (see also supplementary material).

(26) (a) DiSabato, G.; Jencks, W. P. *J. Am. Chem. Soc.* **1961**, *83*, 4400. (b) Kluger, R.; Wasserstein, P. *Biochemistry* **1972**, *11*, 1544.

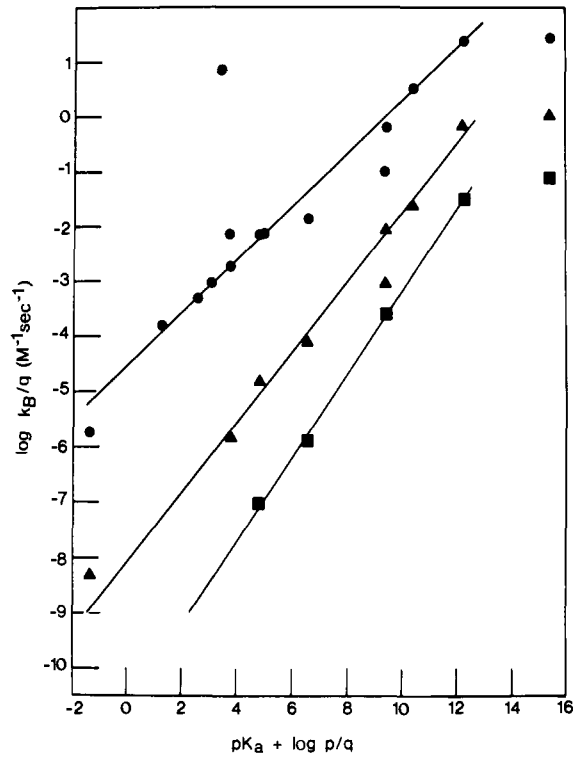

Figure 5. The dependence of the second-order rate constants for the reactions of a series of buffers with isomers **4a**, ●, **3a**, ▲, and **2a**, ■, on the pK_a's of the buffer.

(Acid-catalyzed rates are in Table IX). The results of isotopic labeling show that only phosphorus oxygen bond cleavage is important so all observed reactions involve attack at phosphorus (except **4a** with 24% C–O cleavage for trifluoroethoxide).

The reactivity of an anion toward phosphorus depends upon its basicity with the exception of fluoride and α-effect anions. Fluoride ion is a powerful nucleophile toward phosphorus and is only slightly less reactive than hydroxide. This reaction is an $S_N2(P)$ process and reflects the strength of the P–F bond. In this system fluoride was not found to be a true catalyst for hydrolysis since at room temperature under neutral conditions fluoride reacted with isomers **4a** and **4b** within hours but did not readily hydrolyze to the cyclic diester. In fact only 15% of the fluoro compound hydrolyzed in 2 months at room temperature (via ^{31}P NMR) whereas the 2,4-dinitrophenyl esters would have a half-life of about 4 days at room temperature.

The rate constants for catalysis by oxyanions are correlated by the linear free energy relationships in Figures 5–9. The Brønsted coefficients derived from the linear portion of these plots are given in Table X. It is noted that the Brønsted β_{nuc}'s are the same for each epimer. The β_{nuc}'s are 0.49, 0.64, and 0.75 for 2,4-DNP, PNP, and P esters, respectively. In Khan and Kirby's study of 1,3,2-dioxaphosphorinan-2-ones the corresponding β's were 0.30 and 0.48 for 2,4-DNP and PNP cyclic esters, respectively. Similar β's were also obtained for a related 2,4-DNP phosphate triester by Lazarus and Benkovic[5] and for an acyclic 2,4-DNP phosphate triester by Gorenstein and Lee[10] (Table X). In the Khan and Kirby study only points for acetate, phosphate, carbonate, and hydroxide were used for their Brønsted plot. In our study with more nucleophiles we see that phosphate, carbonate, and hydroxide are all low which accounts for the lower value for their coefficients. The general trends and conclusions fortunately are unaffected but it points out the fact that more kinetic data are always advisable. The point for hydroxide is below the extrapolated linear portion of the Brønsted line as often observed and indicates that there is no additional specific base catalysis. The dianions phosphate and carbonate are low by about 1 order of magnitude for the 2,4-DNP esters. This may be due to the dianionic catalysts binding water more tightly. Thus the dianion is not as free to react via nucleophilic catalysis on the 2,4-DNP esters, and the reaction is

Table V. Rate Constants for the Reactions of Epimer 3a

nucleophile	pK_a	concn range,[a] M	pH[b]	k_B	k_{hyd}[c]
water	−1.59	38.8		3.94×10^{-9} [e]	
methoxyacetate	4.05	0.12–1.0	5.01	4.04×10^{-7}	2.59×10^{-7}
acetate	5.11	0.12–0.98	8.6[d]	4.71×10^{-6}	6.03×10^{-7}
phosphate	6.73	0.037–0.3	7.52	2.21×10^{-5}	1.06×10^{-7}
HF isopropoxide	9.42	0.05–0.4	11.05	2.35×10^{-3}	2.35×10^{-3}
carbonate	9.80	0.015–0.025	10.43	3.52×10^{-4}	5.15×10^{-5}
phenolate	10.39	0.016–0.5	10.97	4.16×10^{-3}	1.05×10^{-4}
TF ethoxide	12.22	0.012–0.05	12.54	0.0815	8.63×10^{-4}
hydroxide	15.4	0.01–0.10		0.119	

[a] Free base. [b] 25 °C, pH of lowest concentration. [c] Intercept. [d] 0.02 M tris buffer. [e] In 1 M KCl, pH 4.3–3.8.

Table VI. Rate Constants for the Reactions of Epimer 4a

nucleophile	pK_a	concn range,[a] M	pH[a]	k_B, M^{-1} s^{-1}	k_{hyd}[c]
water	−1.59	38.8		1.7×10^{-6} [d]	
dichloroacetate	1.59 ± 0.12	0.12–1.0	2.45	8.64×10^{-5}	7.26×10^{-5}
cyanoacetate	2.89 ± 0.07	0.12–1.0	3.77	3.04×10^{-4}	6.85×10^{-5}
chloroacetate	3.32 ± 0.10	0.12–1.0	4.20	4.81×10^{-4}	7.78×10^{-5}
fluoride	3.4[e]	0.002–0.2	8.6[f]	0.769	1.03×10^{-4}
formate	3.98 ± 0.02	0.12–1.0	5.12	5.48×10^{-3}	1.46×10^{-4}
methoxyacetate	4.05 ± 0.05	0.12–1.0	5.01	1.08×10^{-3}	6.61×10^{-5}
acetate	5.11 ± 0.03	0.02–0.4	6.33	3.00×10^{-3}	7.03×10^{-5}
propionate	5.24 ± 0.03	0.12–1.0	6.45	3.08×10^{-3}	6.37×10^{-5}
phosphate	6.73 ± 0.07	0.019–0.3	7.51	3.67×10^{-3}	9.27×10^{-5}
HF isopropoxide	9.42 ± 0.05	0.0025–0.04	11.06	0.485	1.01×10^{-3}
carbonate	9.80 ± 0.21	0.008–0.25	10.46	2.82×10^{-2}	1.32×10^{-3}
phenolate	10.39 ± 0.10	0.005–0.10	10.89	1.35	3.63×10^{-2}
TF ethoxide	12.22 ± 0.17	0.0012–0.01	11.88	3.28	2.40×10^{-3}
hydroxide	15.4	0.0031–0.025	11.9	2.81	

[a] Free base. [b] After reactionat 25 °C, pH of lowest concentration. [c] Intercept. [d] Rate at pH 4/38.8 M. [e] 25 °C, water. [f] 0.02 M tris.

Table VIII. Rate Constants for the Reactions of Epimer 5a

nucleophile	pK_a	5a concn range, M	pH	k_B, M^{-1} s^{-1}	k_{hyd}
phosphate	6.73	0.037–0.3	7.52	1.20×10^{-5}	1.75×10^{-8}
HF isopropoxide	9.42	0.05–0.4	11.06	8.19×10^{-4}	4.72×10^{-4}
phenoxide	10.39	0.016–0.5	10.97	1.06×10^{-3}	5.15×10^{-4}
carbonate	9.80	0.015–0.025	10.43	1.01×10^{-3}	3.28×10^{-4}
TF ethoxide	12.22	0.012–0.05	12.54	0.123	4.95×10^{-3}
hydroxide	15.4	0.005–0.05		0.76	

Table IX. Acid Catalyzed Rate Constant for Epimers

epimer	concn range, M	k_{H^+}
5a	0.01–1.0	8.90×10^{-2} [a]
5b	0.01–1.0	5.43×10^{-1} [a]
4a	0.01–1.0	1.93×10^{-4}
4b	0.01–1.0	9.77×10^{-4}
3a	0.031–1.0	1.02×10^{-5}
3b	0.031–1.0	8.62×10^{-5}
2b	0.125–1.0	6.29×10^{-6}

[a] P-N cleavage.

therefore slower. In the phosphate reaction with the phenyl isomers the point is low but not by nearly as much, indicating that when general-base catalysis becomes a contributing pathway the former effect begins to disappear.

Structure-Reactivity Interactions. A suitable analysis of the structure-reactivity results may be obtained by using a three-dimensional More O'Ferrall/Jencks reaction diagram shown in Figure 10.[27-29] Reactants are in the lower left corner and products are in the upper right. The y axis represents bond formation to the nucleophile, and the x axis represents bond cleavage to the leaving group. If the reaction first proceeds along the y axis and then the x axis, we have a stepwise reaction via a pentacovalent intermediate. If the reaction path is along the diagonal, the reaction is concerted with bond formation to the nucleophile

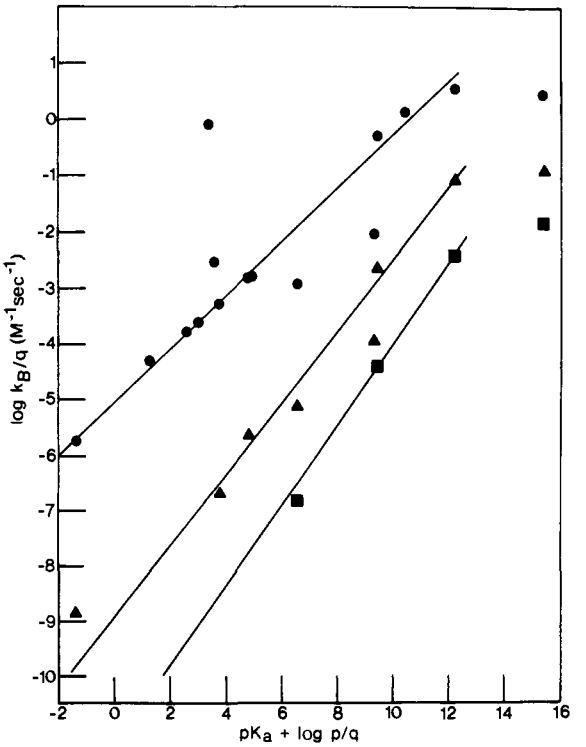

Figure 6. The dependence of the second-order rate constants for the reactions of a series of buffers **4b**, ●, **3b**, ▲, and **2b**, ■, on the pK_a's of the buffer.

(27) More O'Ferrall, R. A. *J. Chem. Soc. B* **1970**, 274.
(28) (a) Jencks, D. A.; Jencks, W. P. *J. Am. Chem. Soc.* **1977**, *99*, 7948. (b) Cordes, E. H.; Jencks, W. P. *Ibid.* **1962**, *84*, 4319.
(29) Jencks, W. P. *Chem. Rev.* **1972**, *72*, 705.

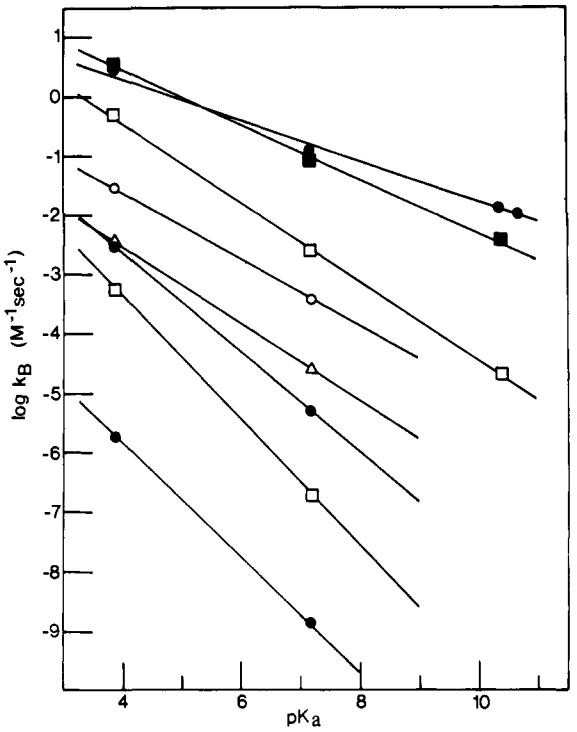

Figure 7. Linear free-energy relationships between rate constants for the attack by anions on the isomers **1a**–**4a** and the pK_a's of the conjugate acids of the leaving groups; OH^-, ●; $CF_3CH_2O^-$, ■; CO_3^{2-}, ○; $(CF_3)_2C$-HO^-, □; HPO_4^{2-}, △; CH_3COO^-, ●; $CH_3OCH_2COO^-$, □; H_2O, ●.

Table X. Brønsted β Values

isomers (leaving group)	β_{nuc} nuc	no. of pts	ref 4	ref 5	ref 10
4b (2,4-DNP)	0.49 (±0.01)	9			
4a (2,4-DNP)	0.48 (±0.02)	9	0.30	0.60, 0.40	0.52
3b (PNP)	0.64 (±0.03)	5			
3a (PNP)	0.64 (±0.05)	5	0.48		
2b (phenoxide)	0.75 (±0.02)	4			
2a (phenoxide)	0.72	3			
5b (PNP)	0.75	3			
5a (PNP)	0.73	3			

base	β_{lg} b isomer	a isomer	no. of pts	ref 4	ref 5
water	−0.79		2	−0.99	−0.82
		−0.96	2		
methoxyacetate	−0.94		2		−0.95
		−1.04	2		
acetate	−0.75		3	−0.88	−0.71
		−0.85	2		
phosphate	−0.62		3	−0.65	
		−0.66	2		
hexafluoro-isopropoxide	−0.58		3		
		−0.64	3		
carbonate	−0.61		2	−0.54	
		−0.57	2		
trifluoroethoxide	−0.44		3	−0.34	
		−0.46	3		
hydroxide	−0.39		4	−0.41	
		−0.35	5		

coupled to leaving group bond cleavage. The β values obtained may be used under certain assumptions to approximate the amount of bond formation or breakage.[28,30] Since β is a correlation between kinetics of transfer of an $(RO)_2PO$ moiety between nu-

(30) Jencks, W. P.; Gilchrist, M. *J. Am. Chem. Soc.* **1969**, *91*, 6066.

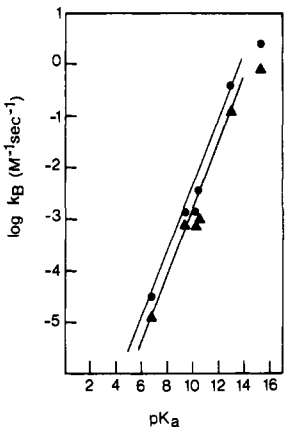

Figure 9. The dependence of the second-order rate constants for the reactions of a series of buffers with isomers **5a**, ▲, and **5b**, ●, on the pK_a's of the buffer.

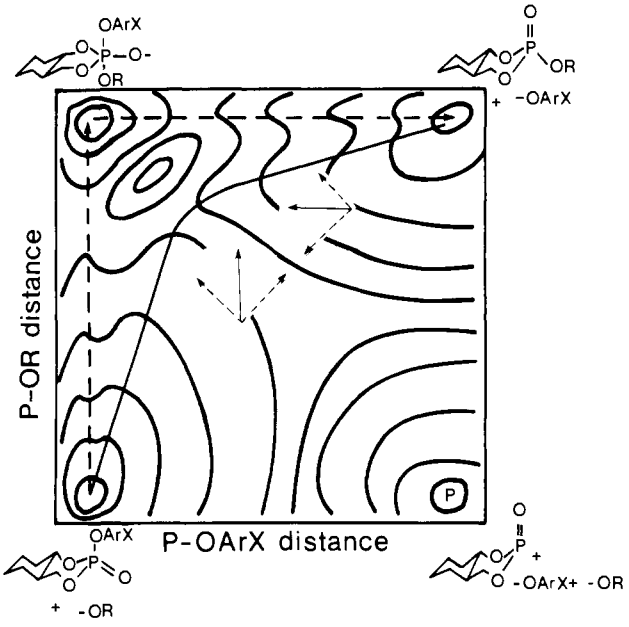

Figure 10. Schematic representation of the potential energy surface for the hydrolysis of phosphate triester.

Table XI. Ratio of Second-Order Buffer Catalyzed Rate Constants, k_B, for b Epimers Relative to a Epimers in Compounds 2–4

	rate ratio (compd) 2b/2a	3b/3a	4b/4a
water			1
dichloroacetate			3.4
cyanoacetate			3.2
chloroacetate			3.5
fluoride			9.6
formate			2.5
methoxyacetate		6.7	3.4
acetate	8.2	6.8	4.4
propionate			4.5
phosphate	8.2	10.3	10.9
HF isopropoxide	5.9	3.5	3.4
carbonate		7.6	10.3
phenolate		5.6	2.5
TF ethoxide	8.7	8.1	6.6
hydroxide	5.5	8.7	9.1

cleophile and leaving group and a proton transfer process, i.e., pK_a, it is necessary to know β_{eq} for equilibrium phosphoryl transfer.

In order to calculate β_{eq} we fitted the data in Tables III–VII (excepting the fluoride, carbonate, and hydroxide points) to the four-parameter equation (3).[4,28b,31] The four unknown a_i coef-

$$\log k_2 = a_1 pK_{1g} + a_2 pK_{1g} pK_{nuc} + a_3 pK_{nuc} + a_4 \quad (3)$$

ficients were obtained by a nonlinear, least-squares computer analysis[10] of the three-variable equation (3). For the **2a**, **3a**, and **4a** esters eq 4 was obtained. For esters **2b**, **3b**, and **4b** the

$$\log k_2 = (-0.977 \pm 0.084)pK_{1g} + (0.0393 \pm 0.0099)pK_{1g}pK_{nuc} + (0.288 \pm 0.060)pK_{nuc} + (-0.998 \pm 0.457) \quad (4)$$

coefficients and linear estimates of the standard deviations are shown in eq 5. Multiple correlations for the four coefficients for

$$\log k_2 = (-0.893 \pm 0.061)pK_{1g} + (0.0333 \pm 0.0077)pK_{1g}pK_{nuc} + (0.346 \pm 0.048)pK_{nuc} + (-0.954 \pm 0.348) \quad (5)$$

each set of esters were 0.98–0.99, and the calculated β_{1g} and β_{nuc} derived from eq 4 and 5 agree very well with those reported in Table X. A symmetry-related multiple-structure-reactivity equation which simply reverses the nucleophile and leaving group labels will describe the reverse reaction k_2 and thus $\log (k_2/k_{-2}) = 0.977\ (pK_{1g} - pK_{nuc}) + 0.288(pK_{nuc} - pK_{1g})$ or $\log K_{eq} = (1.27 \pm 0.14)\ (pK_{nuc} - pK_{1g})$ for the **a** epimers and $\log K_{eq} = (1.24 \pm 0.11)\ (pK_{nuc} - pK_{1g})$ for the **b** epimers. The Brønsted coefficients for equilibrium transfer of $(RO)_2PO$ between nucleophile and leaving group (β_{eq}) is thus 1.2–1.3. A similar value of 1.2 has been estimated for equilibrium transfer of a diester moiety between oxygen nucleophiles and phenolic leaving groups.[31]

For the general case the concerted reaction would have a charge loss from the nucleophile of $\beta_{nuc}/1.2$ and a charge gain on the leaving group of $\beta_{1g}/1.2$ with $\beta_{eq} = \beta_{nuc} - \beta_{1g}$.[32] This implies that over a large range of nucleophiles and leaving groups there should be a gradation of transition-state structures from those resemblimg products to those resembling reactants according to the Hammond postulate.[33,34] The results show that the β_{nuc} increases toward poorer leaving groups and β_{1g} increases toward weaker bases according to the Hammond postulate.

Using the More O'Ferrall/Jencks potential energy surface in Figure 10 and the data in Table X, one may compare the predicted results from raising and lowering the corners of the diagram to the results obtained in Table X. The y axis is defined by β_{nuc} which represents a measure of the phosphorus–nucleophile bond length. If we change the leaving group from a less basic 2,4-DNP to a more basic phenoxide, the energy of the right side of the diagram is raised relative to the left. For a concerted reaction the parallel Hammond effect moves the transition state to the upper right. The anti-Hammond perpendicular effect goes to the upper left. The resultant vector says the β_{nuc} should increase (Figure 10). This follows the observed results. The stepwise pathway would have no change in the position of the transition state, so this interpretation of the results leads one to conclude that the reaction is concerted.

The x axis defined by β_{1g} represents a measure of the phosphorus-leaving group bond length. If we change from a less basic nucleophile such as acetate to a more basic nucleophile such as hydroxide, the bottom of the diagram is raised in energy relative to the top. For the concerted reaction the Hammond effect moves the transition state to the lower left. The anti-Hammond effect is to the upper left, so the resultant vector says the β_{1g} should decrease from acetate to hydroxide (Figure 10). This is the observed result. The stepwise mechanism again would have no Hammond effect and predict no change in the β_{1g}. Thus the results are again consistent with the concerted mechanism.

Finally, since β_{1g} represents a measure of bond cleavage to the leaving group and the β_{eq} is 1.2, a β_{1g} of greater than 0.6 would mean the bond is more than half broken in the transition state. Since only a concerted pathway can have a transition state where

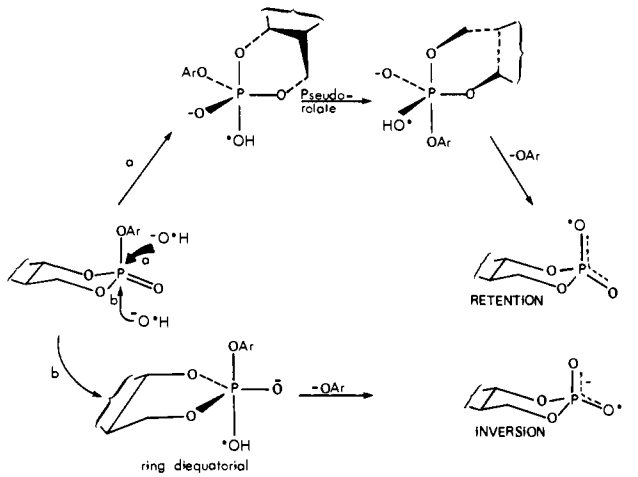

Figure 11. Reaction paths for base catalyzed hydrolysis of axial phosphorinane esters (*O = O-18).

the leaving group bond is mostly broken and the nucleophile phosphorus bond is mostly formed, the reaction path for poor nucleophiles must be concerted.

Unfortunately, a concerted displacement requires the reaction to go via inversion of stereochemistry at phosphorus. The stereochemistry of displacement of the aryl oxide is known for methoxide in methanol[17] and for hydroxide in dioxane/water.[25] The axial epimer **4a** proceeds with 82–83% inversion for both methoxide and hydroxide displacement. Methoxide displacement for the equatorial epimer **1b** proceeds with 91% retention while 41% retention is observed in the hydroxide reaction. Only compound **4b** reacts with 100% inversion of configuration with methoxide while all other triesters react with 4–83% inversion of configuration. For these reactions the retention pathway is generally viewed as involving formation of a pentacoordinate intermediate. The intermediate then pseudorotates and the aryloxy group leaves (Figure 11, path a). The inversion pathway (path b, Figure 11) presumably involves direct backside displacement of the aryloxy leaving group, which requires that the oxygens of the six-membered ring go diequatorial. If this pentacovalent species is a true intermediate, then loss of the leaving group is faster than pseudorotation which would otherwise allow epimerization at phosphorus.

Thus, the reaction stereochemistry shows than an intermediate must exist for very basic nucleophiles in all the reactions (except possibly for **4b**). With good nucleophiles and good leaving groups such as 2,4-DNP the apicophilicity is strong enough to overcome a small energy barrier to placing the ring diequatorial and inversion results.[35,36] With poorer leaving groups such as PhO^- the ring goes apical–equatorial and the intermediate pseudorotates before loss of the leaving group.

The reaction giving retention with good nucleophiles such as hydroxide and methoxide may be explained in Figure 10 by assuming that the β_{1g} sensitivity to hydroxide attack of –0.35 is small enough to mean the attack step follows the potental energy diagram along the left edge. There may be two possible paths the reaction may take, depending on the apicophilicity of the leaving group. The more apicophilic the leaving group, the lower the energy is for the concerted path. The less apicophilic the leaving group, the lower the energy is for the stepwise path. Then from the rest of the kinetic data it could be argued that the concerted path becomes more likely to be followed with less basic nucleophiles. By the time β_{1g} becomes larger than 0.6 the reaction would have to be concerted. A potential energy contour map consistent with the results so far is constructed in Figure 10. This diagram models mechanistic pathways which can rationalize both the stereochemical and kinetic results in terms of a dualty of mechanisms. The concerted path (solid line, Figure 10) is followed

(31) Bromilow, R. H.; Kahn, S. A.; Kirby, A. J. *J. Chem. Soc. B* **1971**, 1091.
(32) Gresser, M. J.; Jencks, W. P. *J. Am. Chem. Soc.* **1977**, *99*, 6963.
(33) Hammond, G. S. *J. Am. Chem. Soc.* **1955**, *77*, 334.
(34) Jameson, G. W.; Lawlor, J. M. *J. Chem. Soc.* **1970**, 53.
(35) Gorenstein, D. G.; Westheimer, F. H. *J. Am. Chem. Soc.* **1967**, *89*, 2762.
(36) Gorenstein, D. G. *J. Am. Chem. Soc.* **1970**, *92*, 644.

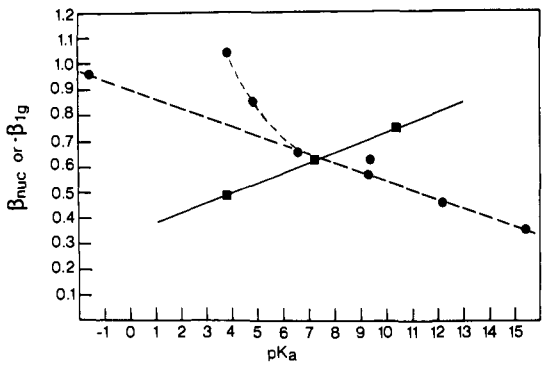

Figure 12. Brønsted β_{nuc} vs. pK_{lg} (solid line, ■) and β_{lg} vs. pK_{nuc} (dashed curve, ●) for the axial epimers.

for good leaving groups and weakly basic nucleophiles while the stepwise path (dashed line, Figure 10) is followed by poor leaving groups and strongly basic nucleophiles.

This unprecedented change in mechanism from a concerted to a stepwise reaction is supported by structure-reactivity relationships between β_{nuc} and pK_{lg} and also β_{lg} and pK_{nuc} (Figure 12). The slope of these lines is called the Cordes coefficient[28b] and is given by

$$-\frac{\partial\beta_{lg}}{\partial pK_{nuc}} = \frac{1}{c_2} = \frac{\partial\beta_{nuc}}{\partial pK_{lg}}$$

For the axial triesters

$$-\frac{\partial\beta_{lg}}{\partial pK_{nuc}} = 0.036 = \frac{1}{c_2} = \frac{\partial\beta_{nuc}}{\partial pK_{lg}} = 0.037$$

For the equatorial triesters

$$-\frac{\partial\beta_{lg}}{\partial pK_{nuc}} = 0.040\ \frac{1}{c_2} = \frac{\partial\beta_{nuc}}{\partial pK_{lg}} = 0.030$$

These least-squares slopes leave out points for acetate and methoxyacetate, and it is potentially significant that in the plots of β_{lg}, the values for acetate and methoxyacetate are significantly higher than the line obtained from hydroxide through phosphate.

By definition the Cordes coefficient is the second derivative of eq 3 with respect to pK_{nuc} and pK_{lg} and is thus the a_2 coefficient. For the axial epimers (using eq 4) $a_2 = 1/c_2 = 0.0393 \pm 0.0099$ and for the equatorial epimers (using eq 5) $a_2 = 1/c_2 = 0.0333 \pm 0.0077$, in excellent agreement with the slopes obtained from Figure 12. The change represented by the break in the plots of Figure 12 (dashed curve) could be due to a transition on the potential energy diagram in Figure 10 where the energy of the concerted pathway is now favored. Thus one is going from the stepwise mechanism, as occurs at least some of the time for basic nucleophiles, to a concerted mechanism for the weakly basic nucleophiles acetate and methoxyacetate.

Stereoelectronic Effects. Deslongchamps and co-workers[37] have established that the orientation of lone pairs controls the decomposition of tetrahedral carbon species. In this stereoelectronic theory cleavage of specific bonds is facilitated by antiperiplanar (app) lone pairs on directly bonded oxygen or nitrogen atoms. Lehn and Wipff[11] and Gorenstein et al.[12-16] have proposed that similar stereoelectronic effects control the hydrolysis of phosphate esters based upon molecular orbital calculations. Unfortunately for the test of the stereoelectronic theory it is now recognized that low-energy twist-boat conformations exist in equilibrium with the chair forms even in the *trans*-decalin-type systems.[17] (See also related twist structures in ref 38–40.) Thus, on the basis of earlier

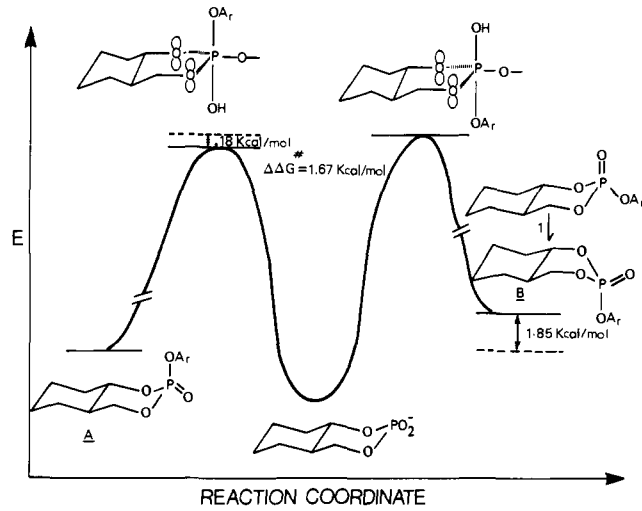

Figure 13. Reaction diagram for hydrolysis of epimeric phosphorinanes. Numbers for **4a**/**4b** at 30 °C from ref 17.

^1H NMR coupling data and ^{31}P and ^{13}C NMR data, the axial aryloxy isomers **1a–5a** of these six-membered ring phosphorinanes are in chair conformations.[17] However, NMR and IR data support the assignment of a twist-boat conformation **6** for "equatorial" epimers **4b** and **5b** and mixed chair twist-boat (50%) for the other epimers **1b–3b**.

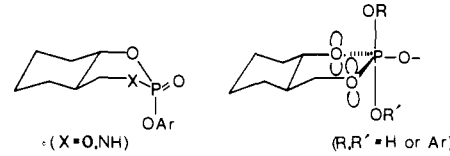

It was earlier suggested that the faster rate of hydroxide-catalyzed hydrolysis for the "equatorial" epimers **1a–5a** was due to ground-state destabilization in the **b** epimers **1b–5b**. Equilibration of the epimeric triesters established that the **b** epimer was ~2 kcal/mol destabilized relative to the **a** epimer, which is close to the difference in free energies of activation (Table I and ref 18).

In fact as shown in Figure 13 the difference in the transition-state energies for the hydrolysis for the 2,4-DNP epimers is less than 0.2 kcal/mol. This suggested that both epimers of **4** have similar transition-state geometries: likely half-chair, diequatorial ring trigonal-bipyramid **7**. The p orbitals on the endocyclic oxygens can most effectively overlap with the apical phosphorus p orbital and both incoming nucleophile and leaving groups. The unusual conformational freedom of the **b** epimers with low energy twist boat structures **6** effectively prevented a direct test of the stereoelectronic theory: in *both* epimeric series **1a–5a** and **1b–5b** (assuming twist structures **6** for the **b** epimers) the ring oxygen (or nitrogen) lone pairs are antiperiplanar to the OAr leaving group.

Important questions left unanswered in the earlier study were the nature of the rate-determining step and the detailed mechanism of reaction which would affect these conclusions. Previous molecular orbital calculations[14,15] suggested that the magnitude of the rate acceleration expected from any steroelectronic effect would depend upon whether the lone pairs were app to the translating bond in the rate-determining step. If nucleophilic attack was rate determining, then the optimal stereoelectronic conformation for facilitating bond making is quite different from that facilitating bond breaking. The lone pairs must be app to the leaving group in the bond-breaking step but app to the *attacking* group in the bond-making step. The attractiveness of transition-state **7** is that this problem is eliminated, since the lone pairs nicely overlap with both groups. It requires a concerted mechanism with coupled bond making and breaking. However, as analyzed in the multiple-

(37) Deslongchamps, P.; Taillerfer, R. J. *Can. J. Chem.* **1975**, *53*, 3029 and references cited therein.
(38) Mosbo, J. A. *Org. Magn. Reson.* **1978**, *6*, 281.
(39) Bajwa, G. S.; Bentrude, W. G.; Pantaleo, N. S.; Newton, M. G.; Hargin, J. H. *J. Am. Chem. Soc.* **1979**, *101*, 1602.
(40) Hutchins, R. O.; Maryanoff, B. E.; Castillo, M. J.; Hargrave, K. D.; McPhail, A. T. *J. Am. Chem. Soc.* **1979**, *101*, 1600.

structure-reactivity correlation section, the buffer-catalyzed hydrolysis of **1-5** represent a continuum of mechanism from concerted to stepwise.

It is possibly quite significant that the rate ratio for the buffer-catalyzed hydrolysis of the two epimers varies from 1 to 10.9 at 70 °C (Table V). At lower tempertures, the k_b/k_a ratio is even larger (up to 37.5 for hydroxide-catalyzed hydrolysis of **4** at 0 °C). This fairly large sensitivity of the rate ratio to temperature is attributable to the favorable enthalpy of activation for **4b** (2.9 kcal/mol lower) and an *unfavorable* entropy of activation for **4b** (3.5 eu more negative than **4a**) (Table I).

The k_b/k_a buffer rate ratio in Table X varies between 1 and 3.5 for reaction of **4b**/**4a** with buffers having pK's less than 4.05 (excepting fluoride) and varies between 5.5 and 10.3 (excepting hexafluoroisopropoxide with **3**) for reaction of more basic buffers (pK > 5) with epimers of **2** and **3**. We have already suggested that the reaction of strong nucleophiles (or general bases) with phosphates having poor leaving groups such as **2** or **3** should follow a path along the edges of Figure 10. This stepwise path accounts for the net retention of configuration in these reactions *and* the higher k_b/k_a ratios. Thus, the transition states for the **b** and **a** epimers have nearly equal energies so that as explained earlier the faster rate for the **b** epimer is entirely explained by ground-state destabilization. This is shown in Figure 13 for a mechanism with a diequatorial transition state, **7**, which presumably would yield inversion of configuration products. This figure should also be modified to provide for a stepwise mechanism for **1-3** with separate transition states for attack and leaving (the bond length of the two apical groups will be unequal in the two different transition states). The retention pathway (path a in Figure 11) with transition states having the six-membered ring spanning apical and equatorial sites should also be of similar energy for the two epimers.

The concerted pathway through the center of Figure 10c has been suggested for phosphate reactions with weakly basic buffers and good leaving groups (**4** with buffers having pK's $\lesssim$ 4). The low k_b/k_a ratios for these reactions can be explained by transition states that largely *retain* the twist-boat destabilization energy for the **b** epimers.

In a concerted process the transition-state lifetime precludes changes in the conformation of the phosphorinane ring to accommodate the best stereoelectronic interactions for *both* the attacking and leaving groups. The transition-state energy differences between epimers will be about the same as the ground-state energy differences (due to the transition state, twist boat structures) and hence the activation energies for reaction of **4a** and **4b** are comparable, leading to small k_b/k_a ratios.

Conclusions

Together, the stereochemical data, multiple-structure-reactivity relationships, and epimer rate ratios provide the first evidence for a continuum of mechanism for reactions of phosphate triesters. Proof of the existence of this continuum of mechanism from stepwise to concerted will hopefully be provided by future stereochemical studies in progress.

Acknowledgment. Support of this research by NSF and NIH is gratefully acknowledged. We also wish to acknowledge the helpful comments of Bob Young. Purchase of the WP-80 NMR spectrometer was assisted by an NSF department grant and high-field NMR was done at the NIH-supported (Grant RRO1077) NMR regional facility at Purdue.

Supplementary Material Available: Tables IVb, Vb, VII, and VIIIb, rate constants for reactions of epimers **2b**, **3b**, **4b**, and **5b**, respectively, Figure 2, pH-rate profiles for **4a**, **3b**, and **2b**, Figure 4, dependence of the observed pseudo-first-order rate constants for the hydrolysis of **3b** on the concentration of trifluoroethoxide, Figure 8, linear free-energy relationships between rate constants for the attack by anions on the isomers **1b-4b** and the pK_a's of the conjugate acids, and Figure 12b, Brønsted β_{nuc} vs. pK_{lg} and β_{lg} vs. pK_{nuc} for the equatorial isomers (7 pages). Ordering information is given on any current masthead page.

Crystal Structures of Repeating Peptides of Elastin. 1. *N*-(*tert*-Butoxycarbonyl)-L-valyl-L-prolyglycyl-L-valylglycine

Hiroshi Ayato, Isao Tanaka,* and Tamaichi Ashida

Contribution from the Department of Applied Chemistry, Faculty of Engineering, Nagoya University, Chikusa-ku, Nagoya 464, Japan. *Received February 17, 1981. Revised Manuscript Received May 13, 1981*

Abstract: The crystal structure of the pentapeptide Boc-Val[1]-Pro[2]-Gly[3]-Val[4]-Gly[5]-OH, one of the repeating sequences of tropoelastin, has been determined by the X-ray diffraction method. It crystallizes as a monohydrate in space group $P2_12_12_1$ with a = 15.480 (3), b = 21.052 (4), c = 9.387 (2) Å and Z = 4. The molecular structure does not have a β turn as proposed for Boc-Val-Pro-Gly-Val-Gly-OMe in solution but takes a rather extended form at the central part from C′ of Pro[2] to N-H of Gly[5]. The peptide molecules arranged along a 2-fold screw axis are linked by the hydrogen bonds to make an infinite antiparallel β sheet.

Introduction

In this decade, the studies of structure-function correlations of elastin have been developed. In 1973, Gray et al. have determined the amino acid sequences in tropoelastin isolated from aortas of copper-deficient pigs to reveal two basic types of regions: a cross-link region and an extensible region.[1-4] The latter contains repeating sequences such as Val-Pro-Gly-Gly, Val-Pro-Gly-Val-Gly, and Val-Ala-Pro-Gly-Val-Gly. The conformations of these peptides, as well as those of high polymers, in solution have been studied by Urry and his co-workers with NMR.[5-9] They

(1) W. R. Gray, L. B. Sandberg, and J. A. Foster, *Nature (London)*, **246**, 461 (1973).
(2) J. A. Foster, E. Bruenger, W. R. Gray, and L. B. Sandberg, *J. Biol. Chem.*, **248**, 2876 (1973).
(3) L. B. Sandberg, N. Weissman, and W. R. Gray, *Biochemistry*, **10**, 52 (1971).
(4) L. B. Sandberg, W. R. Gray, and E. Bruenger, *Biochim. Biophys. Acta*, **285**, 453 (1972).
(5) D. W. Urry and T. Ohnishi, *Biopolymers*, **13**, 1223 (1974).
(6) D. W. Urry, W. D. Cunningham, and T. Ohnishi, *Biochemistry*, **13**, 609 (1974).

0002-7863/81/1503-5902$01.25/0